Journal of Geophysical Research Solid Earth

Supporting Information for

Does deep non-volcanic tremor occur in the central-eastern Mediterranean basin?

G. M., Bocchini[1], P., Martínez-Garzón[2], R. M., Harrington[1], and M., Bohnhoff [2-3],

[1]Faculty of Geosciences, Institute of Geology, Mineralogy, and Geophysics, Ruhr University Bochum, Bochum, Germany

[2]Helmholtz Centre Potsdam GFZ German Research Centre for Geosciences, Section 4.2 Geomechanics and Scientific Drilling

[3]Institute of Geological Sciences, Free University of Berlin, Berlin, Germany.

Corresponding author: Gian Maria and Bocchini (gian.bocchini@rub.de)

Contents of this file

Introduction

This supplements a detailed description of the cross-correlation envelop method used to search for ambient tremor during the occurrence of aseismic slip transients at the Hellenic Subduction Zone and in the eastern Sea of Marmara, and of the seismic network configuration in the two regions (Text S1). The two regions and the available seismic stations are visible in Figure S1. In Figure S2, we report an example of tectonic tremor detected by using the cross-correlation envelope method used in this study. We run the code, with the same settings we used for the eastern Sea of Marmara (Text S1), using land stations around the Cholame segment of the San Andreas Fault where tremor activity has been widely documented (see manuscript). In Figure S3, we show a burst of

signals recorded by a station in Lipari (Eolian Volcanic Arc, Italy) potentially triggered by Love wave induced ground shaking from the 2011 Tohoku (Japan) earthquake. After careful inspection of the waveforms from one day before to one day after we conclude that signals are likely noise given their continuous occurrence over the inspected period when Signal-to-Noise-Ratio levels are lower. In Figure S4 we show a potentially triggered low frequency event at stations in Stromboli (Eolian Volcanic Arc, Italy) during the surface wave shaking of the 2015 Illapel (Chile) earthquake. We can not confirm the triggered nature of the signal because several similar low frequency events are visible before and after the ground shaking induced by the mainshock. Statistical tests comparing the number of events before and after the mainshock would be needed to support the triggered nature of the signal, but it is not in the scope of this study. In fact, the signal is very likely of volcanic origin given the 100 km depth of the plate interface beneath Stromboli. In Figure S5 we show a potential tremor-like signal observed at seismic stations on Crete (Greece) slightly before the arrival of Love waves from the 2015 Illapel (Chile) earthquake. The observation of the signal when PGV values are significantly lower than 0.01 cm/s suggest its spontaneous rather than triggered nature. No similar signals are observed in the day before and after its detection. Table S1 delineates the complete list of candidate mainshocks used for the analysis of triggered tremor.

Text S1.

We employ the envelope cross-correlation method (Ide, 2012, 2010) for the detection and hypocentral location of tremor signals. Raw daily traces are processed in Obspy as follows: (1) bandpass filtered between 2 and 8 Hz; (2) squared; (3) lowpass filtered below 0.1 Hz; (4) and resampled to 1 Hz. The procedure does not create waveform envelopes *sensu stricto* calculated with the Hilbert transform of original waves, but the difference is negligible and allows for faster processing. Envelope correlation is performed only on horizontal channels where tremor signals are expected to exhibit larger amplitudes. For the eastern Marmara Sea, where a shorter time period (~2 months) was investigated, we test varying half-overlapping windows (2, 3, 5 minutes), correlation thresholds (from 0.5 to 0.7) between stations located <100 km apart, and minimum number of horizontal components (from 5 to 8) at which the correlation threshold should be exceeded. When using shorter time windows (2-3 minutes), we required higher cross-correlation coefficients to be exceeded (0.7) at a higher number of channels (8) to limit the number of false detections. Conversely, when using longer time windows of 5 minutes we require lower cross-correlation coefficients to be exceeded (as low as 0.5) at a smaller number of channels (from 5 to 6). In case of the Hellenic Subduction Zone, where the two aseismic transient lasted about 1 year (~6 months each transient and ~4 months each SSE), we used half-overlapping windows of 5 minutes, and cross-correlation thresholds of 0.6 between stations located <100 km apart to be exceeded at a minimum number of 5 horizontal components.

To mitigate the unwanted effects of outliers, the code employs data outlier rejection algorithms. First, it performs a comparison of epicentral distances and travel times for a pair of stations to determine the initial epicenter, and then it associates the best hypocentral depth to it. In the first step, if the differential time between station pairs is larger than the difference in epicentral distance divided by the minimum S-wave velocity in the assumed structure by a certain threshold (i.e. 3 sec), the differential time data is rejected as an outlier. In the second step, if the error between the observed and calculated differential times for a pair of stations is more than three times larger than their standard deviation, the observed differential time data is rejected, and the hypocentral location is calculated again. The latter procedure is repeated until no differential time data is rejected. The envelope correlation method does not distinguish tremor from ordinary earthquakes, therefore we visually inspect all the detections to identify the nature of the signals. We refer the reader to Ide (2012) for further details on the method.

To allow for the best determination of hypocentral locations and enhance detectability of events, we use local S-wave velocity models. For the eastern Marmara Sea, we use the S-wave velocity model from Karabulut et al. (2011), while for the western segment of the Hellenic Subduction Zone, we use the S-wave velocity model from Kassaras et al. (2016).

We are aware of the limitations of applying such method in our cases of study where very dense station coverage is not available (Fig. 1S) and the intense background activity, especially true for the western segment of Hellenic Subduction Zone, could mask

possible tremor signals. We therefore describe the network configuration in detail to make the reader aware of such possible limitations that mask small amplitude signals, such as tectonic tremor.

In the eastern Marmara Sea, to search for tremor activity possibly associated with the slow slip event starting on June 25, 2016 and lasting for about 50 days (Martínez-Garzón et al., 2019) we had an average number of 10 seismic stations available, including 3 boreholes, in the immediate proximity of the Çınarcık Fault (latitude from 40.5 to 41 and longitude from 28.5 to 30). The average interstation distance within the region is of ~20-25 km with most of the stations located to the south of the Çınarcık Fault, on the Armutlu Peninsula. In the broader area of the Sea of Marmara (latitude from 40.2 to 41.3 and longitude from 26.9 to 31) the maximum number of stations increases up to ~25 while the average interstation distance is ~100 km. We use seismic stations operated by the Kandilli Observatory and Earthquake Research Institute (KOERI, http://www.koeri.boun.edu.tr/new/en), from the Armutlu Network deployment (ARNET, Tunç et al., 2011), from the Disaster & Emergency Management Authority (AFAD) seismic network (https://deprem.afad.gov.tr/), and boreholes from the Geophysical borehole Observatory at the North Anatolian Fault (GONAF) deployment (Bohnhoff et al., 2017). We investigated the time period going from the 2nd of June 2016 to the 30th of July 2016.

To search for ambient tremor evidence during the two slow-slip events in 2014-2015 and 2018 along the western segment of the Hellenic Subduction Zone (Mouslopoulou et al., 2020), we used land stations of the Hellenic Unified Seismic Network operated by the National Observatory of Athens (http://bbnet.gein.noa.gr), the University of Patra (http://seismo.geology.upatras.gr/heliplots), the National and Kapodistrian University of Athens (http://dggsl.geol.uoa.gr/), and one additional station operated by the Technological Educational Institute of Crete (http://gaia.chania.teicrete.gr/uk/). During the 2014-2015 geodetic transient (09/24/2014-03/20/2015), we had available up to 13-14 land stations, deployed on Peloponnese, Zakynthos and Kefalonia (latitude from 36.4 to 38.2 and longitude from 19 to 23.2), with an average interstation distance of ~90-100 km. During the 2018 geodetic transient (05/14/2018-10/25/2018), the number of stations was slightly lower (up to 11-12) and therefore the average interstation distance slightly larger (~95-110 km).

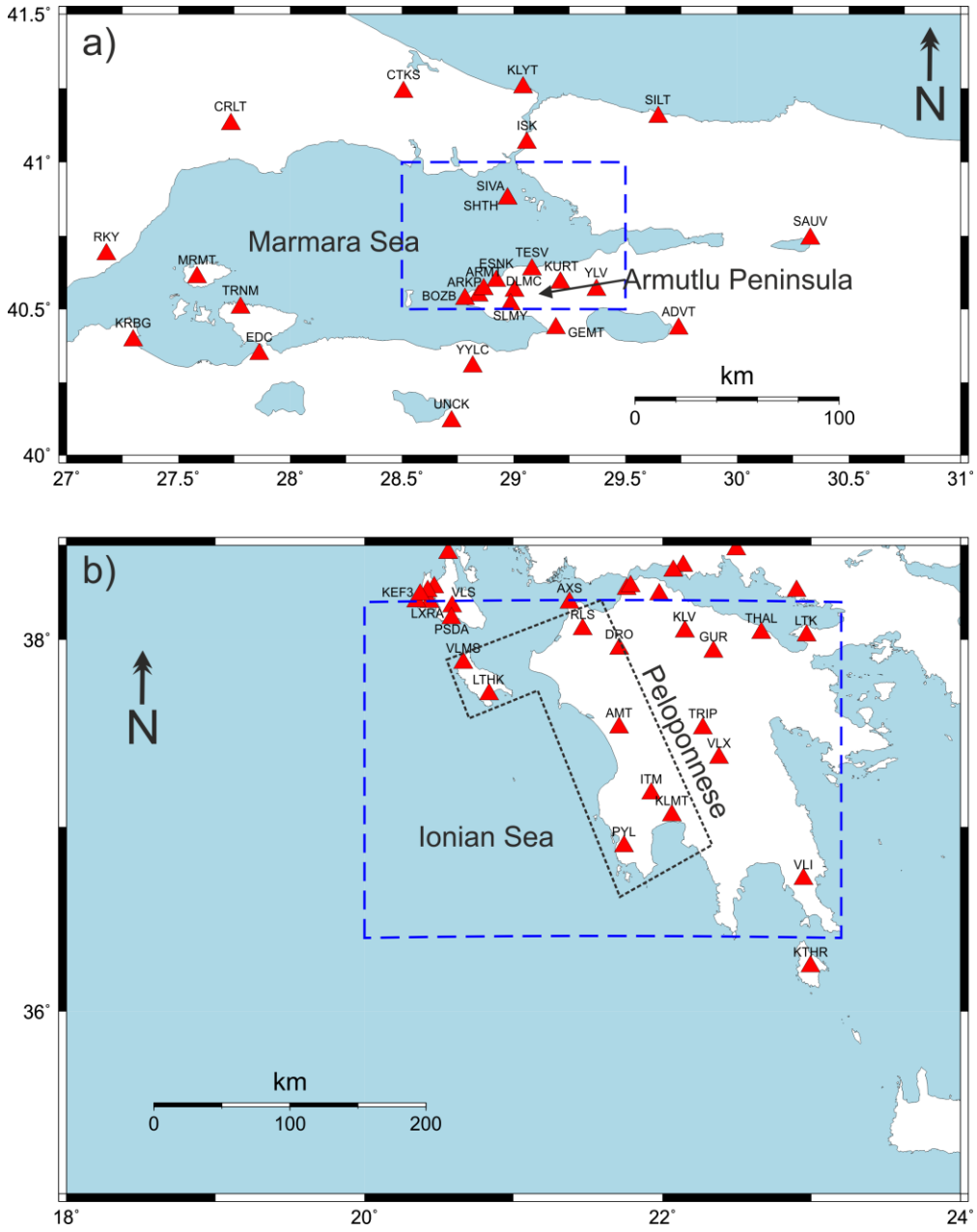

Figure S1. Maximum number of available seismic stations during the occurrence of the slow slip events in (a) the eastern Marmara Sea, and (b) along the western segment of the Hellenic Subduction Zone. The dashed blue boxes surround the closer seismic stations to the slow slip event sources and therefore the region where tectonic tremor would most likely be generated. In the eastern Marmara Sea (a) stations within the dashed blue box have an average interstation distance of 20-25 km, while along the western segment of the Hellenic Subduction Zone (b), stations within the dashed blue box have an interstation distance of 90-110 km. In subfigure b the dashed black line indicates the portion of the plate interface that slipped during the two slow slip events recorded by Mouslopoulou et al. (2020).

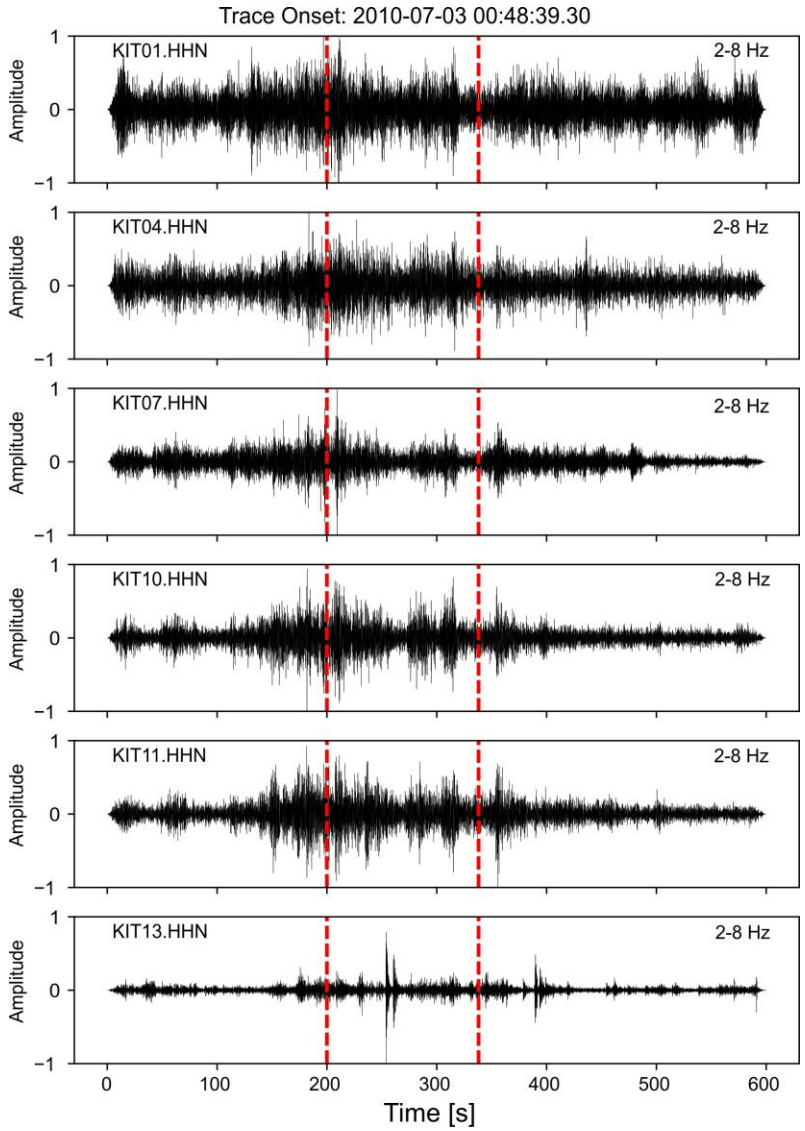

Figure S2. Example of tectonic tremor detected by using the cross-correlation method described in Text S1 and used in this study to detect tremor during documented slow slip events in the central-eastern Mediterranean basin. The signal is detected close to the Cholame segment of the San Andreas Fault, where the occurrence of tremor is widely documented (see manuscript). We used land stations from the Karlsruhe Broadband Array (Horstmann et al., 2013), half overlapping windows of 300 sec and cross-correlation (CC) coefficients of 0.5-0.6 to be exceed at a minimum of 6 components between 0.3 and 100 km apart. We used the same S-velocity model we used for the eastern Sea of Marmara (Text S1). When using a CC coefficient of 0.6 we obtain only the first detection while when lowering the CC coefficient to 0.5 we obtain both the detections shown in the figure. All traces are bandpass filtered between 2 and 8 Hz and time refers to the onset of the trace reported on top of the figure. The detected signal is also reported in the catalog of (Horstmann et al., 2013)

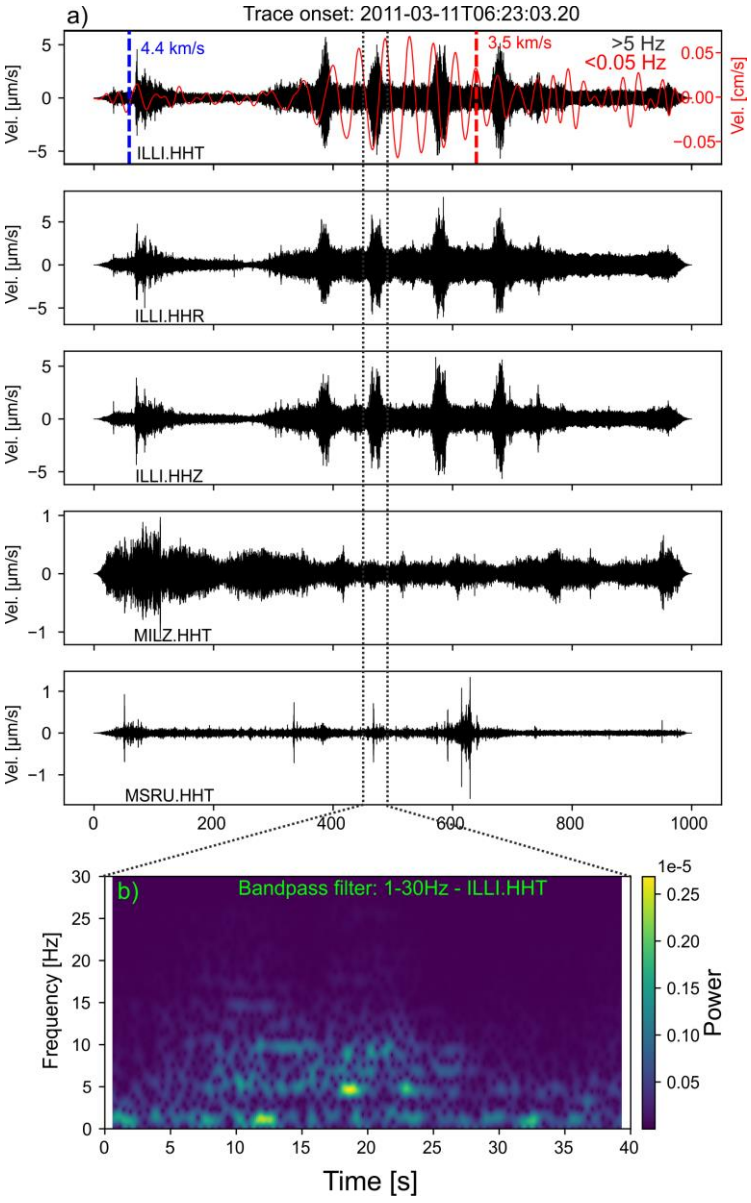

Figure S3. Possible low frequency signal detected at station ILLI (Lipari Island, Aeolian Volcanic Arc, Italy) during the passage of Love waves of the Mw 9.1 11-03-2011 Tohoku earthquake (Japan). The signal is interpreted as noise (see Section 4.1 manuscript). The topmost panel shows overlapping low frequency (<0.05 Hz, red) and high frequency waveforms (>5 Hz, black). (a) The signal is not visible at stations distant about 50 km from ILLI (e.g. MILZ, MSRU). (b) Spectrogram of one of the four bursts showing a frequency content below 10 Hz. The signal window shown in the spectrogram is indicated in the 2nd sub-figure from the top. Dotted blue and red lines in the top panel indicate the predicted arrival time of phases travelling at 4.4 km/s and 3.5 m/s, respectively, used to estimate the arrival time of Love and Rayleigh phases. Figure 2b of the manuscript indicates the station location. The dashed vertical line indicates the time window shown in the spectrogram.

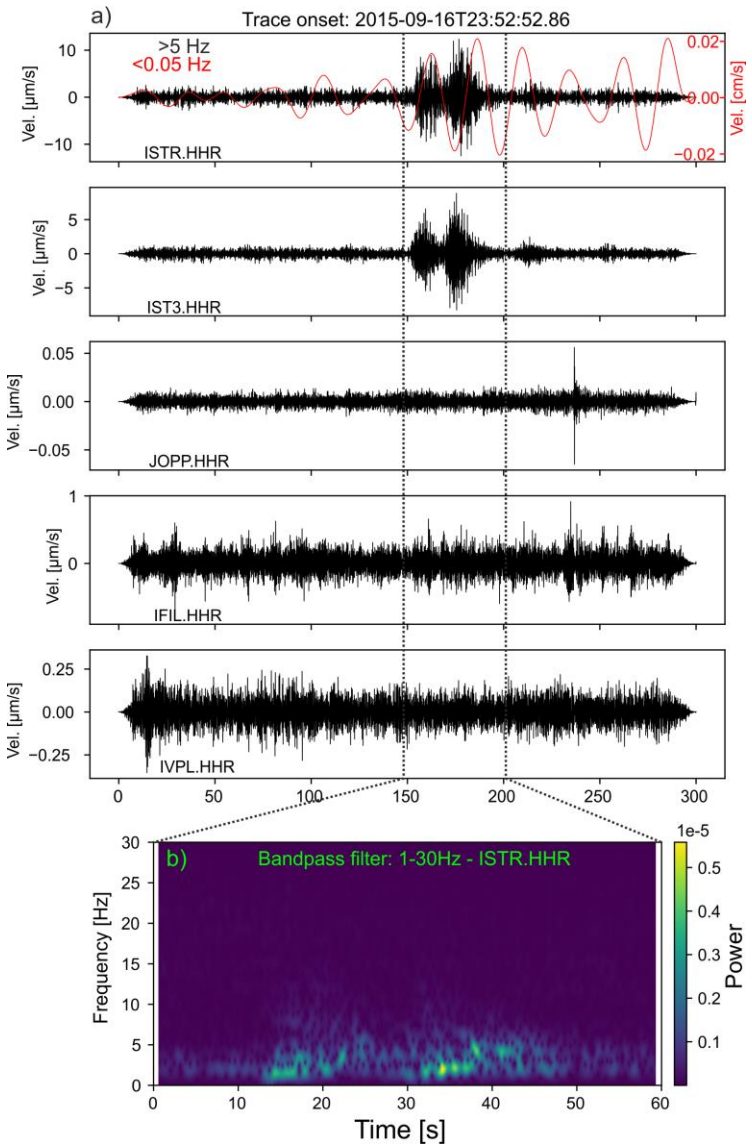

Figure S4. Possible low frequency earthquakes (LFEs) of volcanic origin detected at station ISTR and IST3 (Stromboli Island, Aeolian Volcanic Arc, Italy) during the passage of Rayleigh waves generated from the Mw 8.3 16-09-2015 Illapel earthquake (Chile). The interpretation of the detected signal as triggered event is not straightforward because numerous LFEs occur the day before and after the mainshock (see Section 4.1 manuscript). The top panel shows overlapping low frequency (<0.05 Hz, red) and high frequency waveforms (>5 Hz, black). (a) The signal is not visible at stations > 50 km from Stromboli (e.g. JOPP, IFIL, IVPL), confirming its local origin. (b) Spectrogram of one of the four bursts showing a frequency content below 5-8 Hz. The signal window shown in the spectrogram is indicated in the topmost panel. Figure 2b of the manuscript indicates the station location. The dashed vertical line indicates the time window shown in the spectrogram.

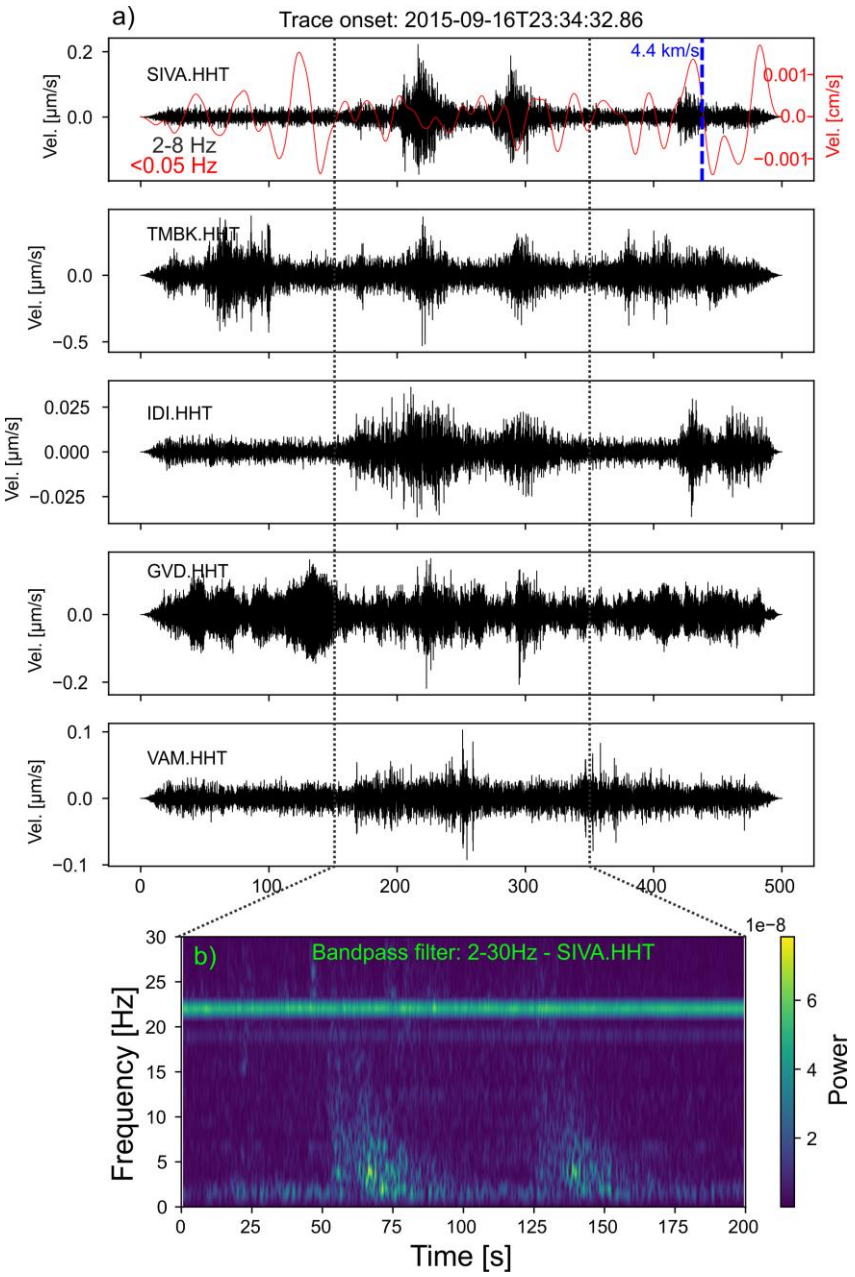

Figure S5. Possible low frequency signals detected at station on Crete before the passage of Love waves generated from the Mw 8.3, 16-09-2015 Illapel earthquake (Chile). The top panel shows overlapping low frequency (<0.05 Hz, red) and high frequency waveforms (2-8 Hz, black). (a) The signal is only visible at nearby stations supporting its local origin. (b) The spectrogram of the observed signal shows a frequency content below 8-10 Hz. The signal window shown in the spectrogram is indicated in the topmost panel. Figure 2c of the manuscript indicates the station location. Notice in the topmost panel the low peak ground velocities (20s period) at the time when the possible low frequency signal is detected. The dashed vertical line indicates the time window shown in the spectrogram.

ID	Date and Time	Fault type	Mw	Lat	Lon	Depth	Where is PGV exceeded	Epicentral Region
1	27/02/2010 06:34:13	T	8,8	-36,1485	-72,9327	28,1	a,b,c,d	Maule, Chile
2	06/04/2010 22:15:02	T	7,8	2,3601	97,1113	33,4	a,c,d	Sumatra, Indonesia
3	25/10/2010 14:42:22	T	7,8	-3,5248	100,104	20,0	-	Sumatra, Indonesia
4	11/03/2011 05:46:23	T	9,1	38,2963	142,498	19,7	a,b,c,d	Tohoku, Japan
5	23/10/2011 10:41:22	T	7,1	38,7294	43,4465	7,6	a,b,c,d	Turkey
6	11/04/2012 08:38:38	SS	8,6	2,2376	93,0144	26,3	a,b,c,d	Sumatra, Indonesia
7	11/04/2012 10:43:11	SS	8,2	0,7675	92,4284	21,6	a,b,c,d	Sumatra, Indonesia
8	11/08/2012 12:23:18	SS	6,5	38,4023	46,838	8,7	d	Armenia
9	28/10/2012 03:04:08	T	7,8	52,6777	-132,172	7,4	a,b,c	British Columbia, Canada
10	24/09/2013 11:29:48	SS	7,8	26,9109	65,5315	15,5	a,b,c,d	Pakistan
11	01/04/2014 23:46:47	T	8,1	-19,6193	-70,7877	17,1	a,b,c,d	Chile
12	24/05/2014 09:25:03	SS	6,9	40,2857	25,4032	28,3	b	Aegean Sea, Greece
13	13/02/2015 18:59:14	SS	7,1	52,5097	-32,0209	16,9	-	Reykjanes Ridge, Atlantic Ocean
14	25/04/2015 06:11:27	T	7,9	28,1302	84,7168	13,4	a	Nepal
15	16/09/2015 22:54:33	T	8,3	-31,5729	-71,6744	22,4	a,b,c,d	Illapel, Chile
16	07/12/2015 07:50:06	SS	7,2	38,2107	72,7797	22,0	c,d	Tajikistan
17	02/03/2016 12:49:48	SS	7,8	-4,9521	94,3299	24,0	a,b,c,d	Sumatra, Indonesia
18	16/04/2016 23:58:37	T	7,8	0,3819	-79,9218	20,6	-	Ecuador
19	30/10/2016 06:40:19	N	6,6	42,8547	13,0884	10,0	c,d	Amatrice, Italy
20	17/07/2017 23:34:14	SS	7,7	54,4715	168,815	11,0	a,b,d	Kamčatka, Russia
21	20/07/2017 22:31:11	N	6,6	36,9643	27,4332	10,2	b	Kos, Greece
22	12/11/2017 18:18:17	T	7,3	34,9052	45,9563	19,0	a,b,c,d	Iran
23	23/01/2018 09:31:43	T	7,9	56,0464	-149,073	25,0	a,b,c,d	Alaska
24	25/10/2018 22:54:53	SS	6,8	37,5148	20,5635	14,0	d	Zakynthos, Greece
25	24/01/2020 17:55:14	SS	6,7	38,3897	39,0883	10,0	a,b,c,d	Turkey
26	28/01/2020 19:10:25	SS	7,7	19,421	-78,7627	14,8	-	Cuba

Table S1. List of initially selected mainshocks to undergo visual inspection for triggered tremor evidence. PGV values are reported in Figure 3 of the manuscript. Focal mechanism solutions are retrieved from the United States Geological Service (USGS, https://earthquake.usgs.gov/) while M_w are from the International Seismological Centre (ISC) catalogue. Letters a, b, c, d in the 8th column indicate in which region the average calculated PGV for each event exceeded the 0.01 cm/s threshold. a) Kefalonia Transform Fault; b) Calabrian Subduction Zone; c) Hellenic Subduction Zone (Crete); d) North Anatolian Fault (eastern Marmara Sea)